Ozone distribution in the lower troposphere over complex terrain in Central Chile

Rodrigo J. Seguel,[1,2] Carlos A. Mancilla,[1] Roberto Rondanelli,[3,4] Manuel A. Leiva,[5] and Raúl G. E. Morales[5]

Received 2 August 2012; revised 8 February 2013; accepted 21 February 2013; published 3 April 2013.

[1] Observations were performed in 12 communities of Central Chile in order to determine the horizontal gradients of ozone in the Santiago Basin and surrounding valleys. Higher ozone mixing ratios were found northeast of the Santiago Basin and included east of the Aconcagua Valley (~70 km from Santiago) suggesting that photochemical pollution produced in Santiago is capable of passing through the Chacabuco mountain chain (~1.3 km) and have impact downwind from the regions with the largest NO_x and VOC emissions. To complement existing surface observations, ozonesonde and tethersonde campaigns were performed in the Santiago Basin and the Aconcagua Valley. The results suggest ozone can accumulate in layers aloft (e.g., >102 ppb at 2 km) similarly to layers observed in complex topography coastal regions like Southern California. Layers of significant ozone concentrations having a near surface origin were observed above the mixed layer and below the subsidence inversion base. We propose that the ozone in this residual layer can be transported large distances (at least to 70 km) to further penetrate into the local environment under conditions of a well-mixed boundary layer.

Citation: Seguel, R. J., C. A. Mancilla, R. Rondanelli, M. A. Leiva, and R. G. E. Morales (2013), Ozone distribution in the lower troposphere over complex terrain in Central Chile, *J. Geophys. Res. Atmos.*, *118*, 2966–2980, doi:10.1002/jgrd.50293.

1. Introduction

[2] Tropospheric ozone is formed from the photochemical oxidation of volatile organic compounds (VOCs) in the presence of nitrogen oxides ($NO_x = NO + NO_2$) [*Jenkin and Clemitshaw*, 2000; *Chameides et al*., 1992; *Atkinson*, 2000]. A typical background ozone concentration at inland sites of the United States and Canada can vary from 25 to 45 parts per billion (ppb) [*Altshuller and Lefohn*, 1996]. The base concentration of surface ozone can increase due to the higher levels of ozone precursors (VOC and NO_x) that are directly emitted to the atmosphere as a result of anthropogenic activities. Typical NO_x emission processes result from the generation of energy (i.e., from thermoelectric plants) and transportation, while the emissions of VOCs are attributed to evaporation losses from liquid fuels, solvents and paints, burning of fossil fuels, and vehicle exhaust. VOCs can also have biogenic sources that may play an important role in urban photochemical smog [*Chameides et al*., 1988].

[3] Ozone can be harmful to human health [*Lippmann*, 1991] and plant life, in addition to causing damage to materials [*Lee et al*., 1996]. Acute exposures to ozone decrease lung capacity, induce inflammations of the respiratory tract, decrease lung defenses, and aggravate preexisting conditions related to the heart and lungs. *McConnell et al*. [2002] found that the incidence of new diagnoses of asthma is associated with heavy exercise in communities with high concentrations of ozone (about 75 ppb as 1 h mean daily maximum); thus, air pollution and outdoor exercise could potentially contribute to the development of asthma in children. *Bell et al*. [2004] found a statistically significant association between short-term changes in ozone and mortality on average for 95 large U.S. urban communities, representing about 40% of the total U.S. population.

[4] For several decades, ozone pollution has been a threat in the central region of Chile, which is characterized by complex terrain and where most of the population of the country and industry are concentrated (Figure 1). Santiago City (33.5°S, 70.6°W) is located in an inland valley in the central region of the country, in between two rivers, Maipo and Mapocho. The city extends over an area of about 1400 km^2 at about 500 m above sea level (asl) and is almost completely surrounded by the Andes mountains to the East (~4.5 km asl) and by the Coastal Range mountains to the West (~1.6 km asl) (Figure 1). The climate in Santiago is of Mediterranean type, with about 300 mm of precipitation per year concentrated during the winter months. Summer local surface circulation is mainly driven by topography and surface radiation. Therefore, Santiago shows a prevalent mountain-valley circulation that controls surface winds and, especially during summer,

[1]National Center of the Environment, Avenida Larraín 9975, CP: 7880096, La Reina, Santiago, Chile.
[2]Now at Department of Atmospheric and Oceanic Sciences, 405 Hilgard Avenue, University of California, Los Angeles, CA 90095-1565, USA.
[3]Department of Geophysics, University of Chile, Santiago, Chile.
[4]Center for Climate and Resilience Research, Santiago, Chile.
[5]Centre for Environmental Sciences, University of Chile, Santiago, Chile.

Corresponding author: Rodrigo J. Seguel, Department of Atmospheric and Oceanic Sciences, 405 Hilgard Avenue, University of California, Los Angeles, CA 90095–1565, USA. (rseguel@atmos.ucla.edu; roseguel@cenma.cl)

2169-897X/13/10.1002/jgrd.50293

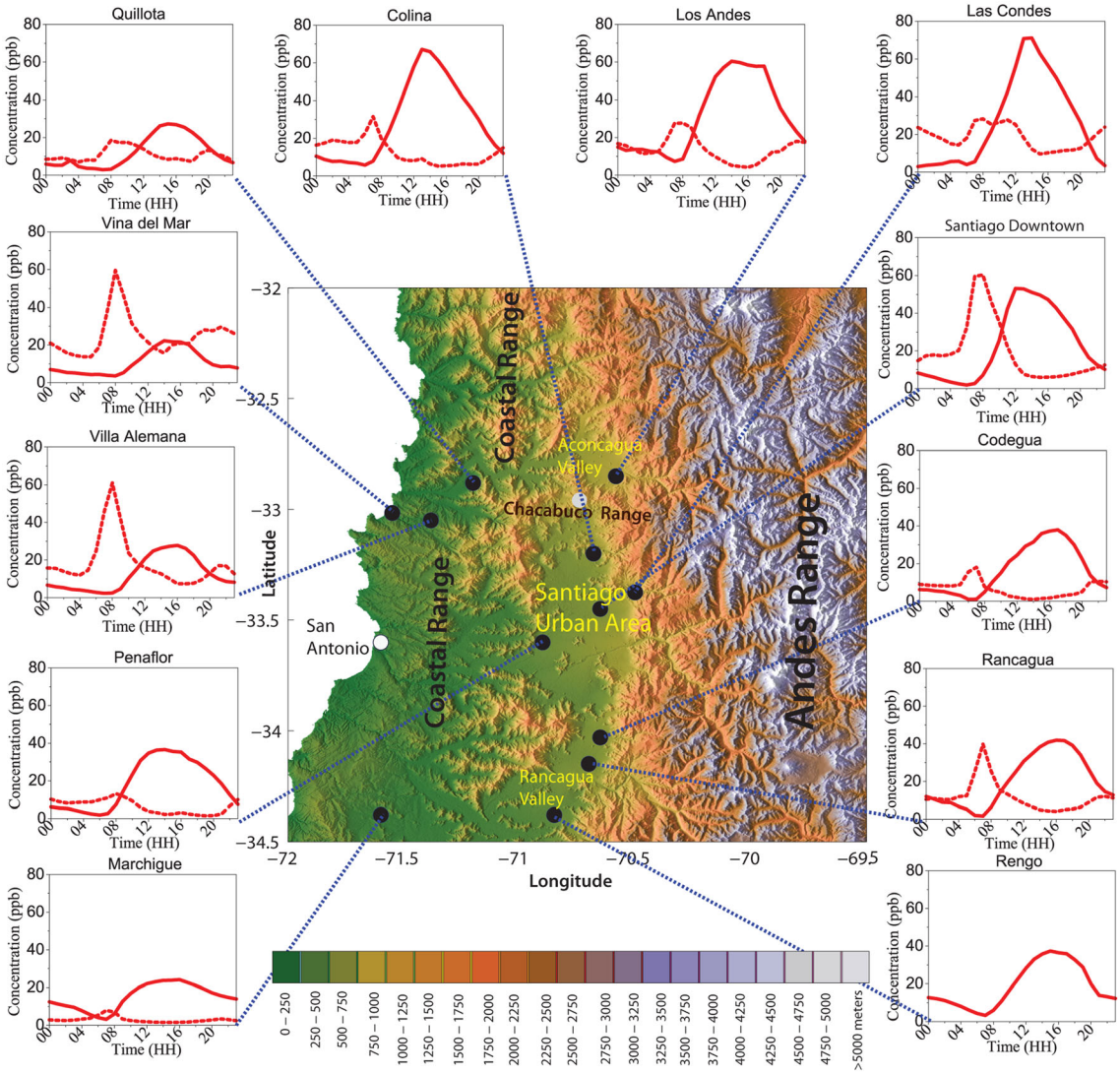

Figure 1. The figure depicts the geographic feature of the central valleys and location of the surface, ozonesonde, and tethersonde (white dot over Chacabuco mountain range) observations. The figure also shows the mean diurnal variations of ozone (continuous lines) and nitrogen oxides (dashed lines) at the Aconcagua Valley station (16 March to 5 April 2010), the Santiago Basin station (15 December 2009 to 4 January 2010), and the Rancagua Valley station (1 February to 12 March 2010).

experience only a minor modulation by the synoptic scale circulations. This secondary influence by the synoptic variability results in small day-to-day variations in surface winds [*Schmitz*, 2005]. Maximum wind speeds occur between 14:00 and 17:00 LT (in this paper, UTC-4 will be used as Local Time) with predominantly southwesterly wind at the time of the day when the mountain-valley circulations are fully developed. The Coastal Range acts as an efficient barrier to isolate the Santiago basin from the direct influence of oceanic air masses. This, together with the large values of surface solar radiation during summertime, results in average maximum temperatures that are 5 to 15°C higher in the Santiago basin than in nearby coastal regions.

[5] In Central Chile, synoptic-scale conditions associated with the formation of photochemical smog are characterized by the presence of a midtropospheric ridge or by the passage of coastally trapped lows, both locally increasing the subsidence in the middle and low troposphere above the mixed boundary layer. Summertime clear skies over Santiago are only occasionally interrupted by the passage of troughs in the middle troposphere, cutoff lows, or, even more rarely, midlatitudes frontal systems.

[6] The urban atmosphere of Santiago is a heavily polluted environment, due to the activity of more than six million people localized in a deep topographical valley on the west side of the Andes (Table 1). During summertime, the larger solar irradiance together with NO_x and VOCs precursors results in a marked rise in ozone levels [*Rubio et al.*, 2004; *Rappenglück et al.*, 2005]. Moreover, *Préndez and Peralta* [2005] have found that photochemical smog can be even more significant in cities like Santiago where biogenic emissions from the abundance of exotic trees may greatly exceed that from native plants.

[7] The urban area of Santiago has historically experienced the most severe ozone pollution in Chile. Levels as high as 174 ppb (1 h) have been measured by the official

Table 1. Population by Region and Communes

Region	Population[a]	Commune	Population[a]
Valparaíso (Aconcagua Valley)	1,539,852	San Antonio	87,205
		Valparaíso (including Viña de Mar commune)	876,022
		Villa Alemana	95,623
		Quillota	75,916
		Los Andes	60,198
Santiago Metropolitan Region (Santiago Basin)	6,061,185	Peñaflor	66,619
		Santiago City (including Santiago downtown and Las Condes)	4,668,473
		Colina	77,815
O`Higgins Region (Rancagua Valley)	780,627	Marchigue	6,904
		Rengo	50,830
		Rancagua	214,344
		Codegua	10,796

[a]2002 last census available.

monitoring network during summertime (17 January 1998 at 14:00 LT). Moreover, the Chilean National Ambient Air Quality Standard (NAAQS) for ozone (61 ppb 8 h average) is currently exceeded on more than one third of the summer days in Santiago [*Seguel et al*., 2012]. Also, day-of-the-week variations in ozone and its precursors have shown that the VOC/NO_x ratios have been significantly higher on Sundays compared with weekdays, allowing higher ozone concentrations on weekends. The increasing VOC/NO_x ratios up to ~6.4 are characteristic of a chemical process limited by VOC [*Seguel et al*., 2012]. However, the observed peak ozone concentrations show large spatial variability. The northeast sector of the city shows the highest ozone levels, whereas the lowest levels are measured in the west and southwest [*Seguel et al*., 2009]. The prevailing winds transport ozone and its precursors to the northeast part of the basin, where higher ozone levels are recorded. However, without automatic monitoring stations further downwind, the spatial extent of the ozone plume cannot be fully determined. This aspect is crucial for downwind regions like Los Andes City, currently an attainment area with no official ozone monitoring network.

[8] In this paper, we focus on determining the horizontal and vertical extent of the transport of ozone and ozone precursors by looking at detailed surface and upper air ozone observations. Although Santiago has been a nonattainment area for O_3 during previous decades, neither vertical profile measurements nor extensive measurements downwind of the Santiago Basin were available, which are needed for interpreting pollutant dispersion and photochemistry within the valley-mountain breeze circulation regime of Santiago. This study analyzes surface observations (i.e., O_3, VOC, and NO_x) and the first vertical ozone measurements in the Santiago Basin and surrounding valleys, which allow us to begin to explore the mechanisms that control regional ozone formation and transport across the basins. Our findings highlight an important aspect of pollution transport, namely, that isolated regions far from the main emission sources in Chile cannot control their pollutant levels by local regulation alone.

2. Materials and Methods

2.1. Surface Observations

[9] In the Santiago Basin, four sites were selected in the towns of Peñaflor (upwind), Central Santiago (downtown), Las Condes (downwind), and Colina (downwind) in accordance with the predominant wind direction during the hours of greatest photochemical activity (Figure 1). In the Rancagua Valley, the stations of Marchigue, Rengo, Rancagua, and Codegua were selected using the same criteria. The town of Marchigue corresponds to a rural location. The Rengo-Rancagua-Codegua transect corresponds to upwind and downwind conditions for Rancagua city. For the Aconcagua Valley (Valparaíso region), the Viña del Mar, Villa Alemana, and Quillota stations were selected to assess the possible impact of the local emissions downwind in the town of Los Andes.

[10] At each site, O_3, NO_x, and surface meteorological variables were monitored continuously. Ozone was determined using continuous monitors based on a UV absorption technique (Thermoscientific Inc. USA, www.thermoscientific.com, Model 49i). This analyzer has a minimum detection limit of 1.0 ppb, a response time of 10 s, and an absolute accuracy of 2%. NO_x was determined using a chemiluminescence analyzer (Thermoscientific Inc. USA, Model 42i). NO_2 is converted to NO by a molybdenum converter heated to ~325°C. This instrument has a minimum detection limit of 1.0 ppb, a response time of 120 s, and absolute accuracy of 1%. For both measurements, the averaging time was 5 min.

[11] Additionally, volatile organic compounds were collected using stainless steel SUMMA-polished canisters. The sampling procedure is based on the pressurized sampling method described by *Zielinska et al*. [1996]. The pressurized canisters (up to 15–20 psi of pressure) were analyzed at the Desert Research Institute organic laboratory in Reno, Nevada, within 1 month of sampling.

[12] The sampling of VOCs was performed during weekdays and weekends at times of high anthropogenic activity (i.e., from 06:00 to 10:00 LT) and in periods with good vertical mixing and intense photochemical activity (i.e., from 12:00 to 16:00 LT). For the Aconcagua and Rancagua Valleys, a third measurement was performed in the late afternoon/evening (i.e., from 18:00 to 22:00 LT) since these areas have been poorly characterized.

2.2. Analysis of Volatile Organic Compounds

[13] Canister samples were analyzed for VOCs using a gas chromatography/mass spectrometry technique according to EPA Method TO-15 [*U.S EPA*, 1999]. The GC-FID/MS system included a Lotus Consulting Ultra-Trace Toxics sample preconcentration system built into a Varian 3800 gas chromatograph with a flame ionization detector, which was coupled to a Varian Saturn 2000 ion trap mass spectrometer.

[14] The system was calibrated using a mixture that contained the most commonly found hydrocarbons (75 compounds from ethane to *n*-undecane, purchased from Air Environmental) in the range of 0.2 to 10 ppb. Three-point external calibrations were run prior to analysis, and one calibration check was run every 24 h. Subsequent analyses were conducted at least 24 h after the initial analysis to allow re-equilibration of the compounds within the canister. The estimated overall uncertainty of VOC measurements was about ±10%.

2.3. Experimental Design of Upper Air Ozone Measurements

[15] The balloon flights were conducted from September 2010 to September 2011. Ozonesonde launches were programmed on a monthly basis at different times of the day (morning, noon and afternoon) in order to capture the daily ozone variations and changes throughout the year. The launches were mostly made from a National Center of the Environment (CENMA) air quality station located in Colina, which was equipped with an ozone analyzer and a NO_x analyzer (both previously described in section 2.1).

[16] In January, a campaign was conducted to study the transport of ozone from the Santiago Metropolitan Region to the city of Los Andes, which is located in the Aconcagua Valley (Figure 1). First, the vertical profile of Los Andes was characterized on 6 January (6:00, 11:00, and 15:00 LT), then San Antonio on 18 January (6:00, 11:30 and 14:00 LT), and finally, during three consecutive days (19, 20, and 21 January), ozonesondes were launched from the Metropolitan Region in the morning (~11:00 LT) and from Los Andes in the afternoon (17:00 LT). Simultaneously, on 19, 20, and 21 January, the concentration of ozone was monitored between 12:00 and 18:00 LT with a tethersonde located at the peak of La Cruz hill, in the Chacabuco mountain range (Figure 1).

[17] The measurements taken in the Colina-Los Andes corridor were supplemented with measurements on 13 January 2011 in Rancagua (6:00, 12:00, and 14:30 LT) and on 22 February 2011 in Peñaflor (6:00, 11:00, and 14:37 LT). Table 2 summarizes the location of the launches and the number of measurements at each location.

2.4. Acquisition of Ozonesonde Data

[18] Ozone profiles were measured using the electrochemical concentration cell (ECC) type (Model 6A ECC, Science Pump Corporation). A total of 40 ozonesondes were launched at different sites (Table 2) using 1.2 kg rubber balloons (Totex). The ascent rates of these balloons were typically 3–6 m/s with burst altitudes in the range of 30–35 km. The transmitted data were received by a ground based 400–406 MHz receiver at a 1 s interval. The ECC sensor consists of Teflon cathode and anode chambers containing platinum electrodes immersed in KI solutions of different concentrations. The concentration of KI solution in the sensor cathode chamber was 1%. For this type of sonde, *Smit et al*. [2007] found biases <5%, a precision of 3–5%, and an accuracy of 5–10% up to 30 km. As a control, before every flight, prelaunch comparisons were made between ozonesonde readings and surface analyzer readings (Thermoscientific Inc. Model 49i) at the corresponding station. If the ECC reading disagreed with the surface monitor by more than 10%, the ECC was changed.

[19] Pressure, temperature, and relative humidity (RH) measurements were recorded by Vaisala RS92-SGP radiosondes. The calibration of the pressure, temperature, and humidity sensors was performed with the Vaisala Ground Check Set GC25. Each sonde's global positioning system (GPS) provided latitude, longitude, altitude, wind speed, and wind direction data.

2.5. Tethersonde Measurements

[20] Tether balloon measurements were obtained at the peak of La Cruz hill, located in the Chacabuco mountain range. The system consisted of a tethered balloon (Vaisala TTB329; 7 m^3 in volume) coupled with a compact (9×21 29 cm) and lightweight (0.7 kg without casing) ozone monitor (2B Technologies Inc., Model 205), which measures UV absorbance at 253.7 nm. This analyzer has a minimum detection limit of 2.0 ppb, a response time of 4 s, and accuracy of 2%. The arrangement, controlled by an electric winch, allowed reaching an elevation of 200 m above ground level.

2.6. Mixed Layer Height Identification

[21] The sonde variables were used to assess mixed layer (ML) heights as described by *Morris et al*. [2010, and references therein]; the temperature inversion; the potential temperature θ, which is nearly constant in a well-mixed boundary layer [*Nielsen-Gammon et al*., 2008]; and the sharp decrease in RH which frequently marks the top of the ML. Finally, the ozone profiles also show evidence of

Table 2. Measurement Periods of O_3, NO_x, and VOCs at Surface Level and Launching Points of Ozonesondes

Monitoring Station	Latitude (S)	Longitude (W)	Altitude (m asl)	NO_x and O_3	VOC Speciation	O_3 Sounding
San Antonio	33°36′09″	71°36′52″	16	-	-	3
Viña de Mar	33°01′13″	71°33′00″	19	16 Mar to 5 Apr 2010	17, 18, 21, 24, 25 Mar 2010	-
Villa Alemana	33°03′19″	71°23′27″	145	16 Mar to 5 Apr 2010	17, 18, 21, 24, 25 Mar 2010	-
Quillota	32°53′27″	71°12′35″	138	16 Mar to 5 Apr 2010	24, 25 Mar 2010	-
Los Andes	32°50′45″	70°35′12″	839	16 Mar to 5 Apr 2010	17, 18, 21, 24, 25 Mar 2010	6
Peñaflor	33°36′02″	70°54′02″	377	15 Dec 2009 to 4 Jan 2010	16, 17, 20, 23 Dec 2009	3
Santiago downtown	33°27′40″	70°39′29″	540	15 Dec 2009 to 4 Jan 2010	16, 17, 20, 23 Dec 2009	1
Las Condes	33°22′26″	70°31′21″	795	15 Dec 2009 to 4 Jan 2010	16, 17, 20 ,23 Dec 2009	3
Colina	33°12′21″	70°41′06″	582	15 Dec 2009 to 4 Jan 2010	16, 17, 20, 23 Dec 2009	21
Marchigue	34°23′49″	71°36′56″	140	1 Feb to 12 Mar 2010	7, 9, 10, 11 Mar 2010	-
Rengo	34°23′40″	70°51′11″	330	1 Feb to 12 Mar 2010	7, 9, 10, 11 Mar 2010	-
Rancagua	34°09′44″	70°42′50″	515	1 Feb to 12 Mar 2010	7, 9, 10, 11 Mar 2010	3
Codegua	34°02′03″	70°39′46″	559	1 Feb to 12 Mar 2010	7, 9, 10, 11 Mar 2010	-

the location of the ML: the ozone concentration within the ML is nearly constant [*Zhang and Rao*, 1999], while a sharp ozone gradient frequently occurs at the top of the ML [*Athanassiadis et al*., 2002]. For example in Figure 2, the gradient in the temperature profile shows a clear change at ~2.5 km, while the potential temperature is almost constant at ~295 K from the surface up to ~2.5 km. Relative humidity (RH) increases steadily from the surface up to ~2.5 km, where a sharp negative gradient occurs. The ozone profile depicts a nearly well-mixed layer from the surface up to ~2.5 km, with $O_3 > 38$ ppb at the surface, increasing to 50 ppb from 0.6 km to 2.5 km, then decreasing rapidly back to near surface values at ~2.5 km.

2.7. Residual Layer Identification

[22] The collapse of the ML after sunset leaves part of the material entrained by the convective boundary layer trapped overnight and can be potentially re-entrained the next day when a new convective boundary layer develops [e.g., *Neu et al*., 1994]. It is also possible, however, for residual layers to be advected downwind. Thus, photochemically aged plumes containing high levels of ozone, precursors, and aerosol particles can be transported within the residual layer (RL) with little dilution and adversely affect the air quality of regions several hundred kilometers downwind the next day [*Zaveri et al*., 2010]. Above Santiago, the top of the RL is marked by a capping subsidence inversion and sharp RH gradients, and the ozone concentrations reach values that remain nearly constant. For the case shown in Figure 3, the base of the RL is found just over 1.4 km, where the temperature profile depicts an inversion and the vertical gradient in θ increases. RH shows a steep decrease at the same level, while ozone experiences a rapid increase up to a maximum near the top of the RL, just below 2.5 km.

2.8. Back Trajectories

[23] Three-dimensional back trajectories were calculated for one case study from 18 to 20 January 2011. We used the Weather Research Forecast (WRF) model to simulate the wind fields during that period. WRF is a numerical model that solves the fully compressible nonhydrostatic

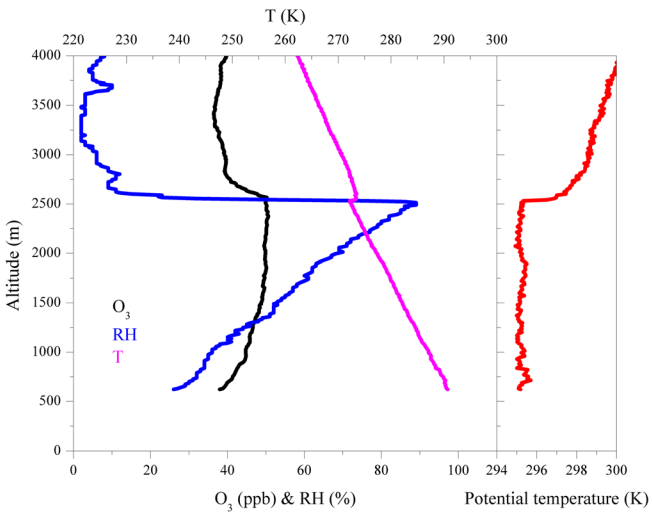

Figure 2. Example of ML identification methodology using sonde data from 29 September 2010 (14:00 LT) at Colina.

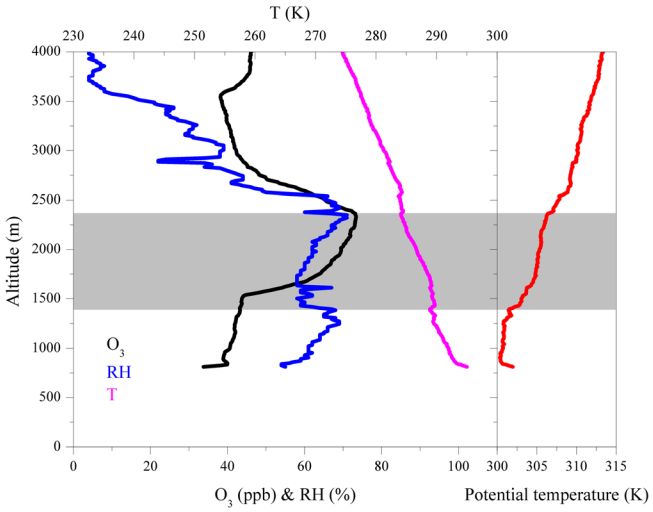

Figure 3. Example of RL identification methodology using sonde data from 23 February 2011 (11:00 LT) at Las Condes. The gray zone indicates the RL.

equations in a terrain following mass vertical coordinate system [e.g., *Skamarock et al*., 2007]. The model was run using two nested domains, the smaller one having a horizontal resolution of ~6 km and 50 eta levels in the vertical, with 10 eta levels located lower than 0.9 (about 900 hPa) and with a top pressure of 50 hPa. Physical parameterizations most relevant for the calculation of the back trajectories are the Mellor-Yamada-Janjic parameterization of the boundary layer [*Janjić*, 1994], the Pleim-Xiu land surface model [*Pleim and Xiu*, 1995], and the Rapid Radiation Transfer Model radiation schemes [*Clough et al*., 2005]. The trajectory calculation is performed using a time step of about 2 min. That is, every 2 min, a new position for the given particle is calculated, interpolating the winds in space and time (both horizontally and vertically using the model omega velocity) and for about 8 h in total. If the trajectory parcel reaches the surface at some point, then it continues to be advected at the surface level using the surface wind. Given the observational focus of this work, we have used this approach as it is the simplest that provides a first idea on the plausibility of the across-valley transport through the Residual Layer (RL).

3. Results and Discussion

3.1. Overview of O_3-NO_x-VOC

[24] Monitoring was performed in several valleys that were separated by mountain ranges, and the relationship between the trace gas levels in each valley is discussed in terms of the relative contribution of local emissions and transport between the valleys.

3.1.1. Valparaíso Region (16 March to 5 April 2010)

[25] Los Andes, currently an attainment area without official ozone monitoring measurements, is affected by elevated ozone levels which are not locally produced. Furthermore, our measurements distinguish Los Andes from other important precursor sources located in the valley. Indeed, the highest concentrations of NO_x were recorded at the Viña del Mar and Villa Alemana stations. Furthermore, during the measurement periods, the highest VOC concentrations were observed in Villa

Table 3. VOC Morning Average (6:00–10:00 LT) at the Monitoring Stations

Monitoring Station	Average Value (ppbC) ± Standard Deviation	Maximum (ppbC)	Minimum (ppbC)	n^a
Viña de Mar	38.7 ± 9.2	49.8	25.1	5
Villa Alemana	55.9 ± 27.2	93.8	21.8	5
Quillota	16.7 ± 1.6	17.9	15.6	2
Los Andes	18.2 ± 9.0	33.4	10.8	5
Peñaflor	22.7 ± 8.8	35.2	15.6	4
Santiago Downtown	71.5 ± 55.4	125.2	14.5	3
Las Condes	47.8 ± 36.7	102.2	24.0	4
Colina	41.5 ± 13.1	56.6	26.7	4
Marchigue	9.2 ± 7.7	20.1	3.4	4
Rengo	17.4 ± 11.1	27.6	6.9	4
Rancagua	30.4 ± 11.1	44.4	17.5	4
Codegua	17.1 ± 4.2	21.1	11.9	4

[a]Number of evaluated analyses above detection limit.

Alemana between 6:00 and 10:00 LT (Table 3). However, Los Andes, located in the eastern part of the Aconcagua Valley, showed a higher O_3 concentration (Figure 1). The maximum O_3 values generally occurred between 14:00 and 18:00 LT when the stronger surface winds were recorded in the Valparaíso Region (~4 m/s) showing a predominant southwesterly direction. The most striking feature of the ozone observations at Los Andes is the widening in the mean diurnal cycle of ozone observed after 17:00 LT, suggesting that Los Andes could be a receptor site for ozone pollution, either from activity in the cities near the coast or from the Santiago basin. However, surface ozone measurements at Los Andes cannot explain by themselves where the ozone is coming from, which will be discussed in detail in the next sections. During the monitoring period, the 8 h average O_3 concentration at Los Andes exceeded 61 ppb on 11 occasions (55% of the days). In contrast, the maximum O_3 levels never exceeded 40 ppb at Viña del Mar, Villa Alemana, and Quillota due to the sea breeze bringing cleaner air from the Pacific ashore.

3.1.2. Santiago Basin (15 December 2009 to 4 January 2010)

[26] Elevated O_3 levels were found in the Santiago Basin after air masses have incorporated more precursors during transport across the city. The highest NO_x and VOC concentrations occurred at the downtown Santiago station. An intense peak in the NO_x level was observed at approximately 7:00 LT. In Las Condes, NO_x concentrations were at about half of the levels measured in downtown Santiago. In addition, two maxima were observed at approximately 8:00 and 11:00 LT in Las Condes (Figure 1). Since during daytime hours southwesterly winds transport polluted air masses to Las Condes [*Rappenglück et al*., 2000], it is possible that NO_x arrival from downtown may contribute to this second maximum, although, due to the lifetime of NO_x (hours to days), this contribution could be minor. Thus, we believe this second maximum is also the result of the intense traffic emissions which in fact take place at midday in this busy area of the city. Consequently, Las Condes is not only a receptor site but also an important source of primary pollutants unlike the case of Colina and Los Andes.

[27] The mean diurnal variations of O_3 (Figure 1) showed that the highest concentration occurred in the central and northeastern parts of the Metropolitan Region (Las Condes, Colina, and downtown Santiago). For example, in Las Condes and Colina, the 8 h average O_3 concentration often exceeded 61 ppb. In comparison, Peñaflor, being at the southwestern entrance of the valley, had relatively low O_3 concentrations. This suburban location can be considered to be the background concentration for the Santiago Basin. Measurements in Peñaflor are particularly important for the Santiago Basin because at this location the Coastal Range, which has altitudes of greater than 1.2 km asl, has a 50 km-wide gap that contains the Maipo River. This gap, together with predominant southwesterly winds, makes this zone the entryway for "fresh" air to the city of Santiago.

[28] In the Santiago Basin, the highest wind speeds occurred between 14:00 and 20:00 LT (2–6 m/s), with predominant westerly winds in Peñaflor. The winds were southwesterly in downtown Santiago, west-southwesterly in Las Condes, and south-southwesterly in Colina during this highest period of ozone formation.

3.1.3. Rancagua Valley (1 February to 12 March 2010)

[29] Current measurements of trace gas levels in Rancagua Valley are the lowest encountered in the three valleys. VOC concentrations were generally low and did not surpass 45 ppbC (Table 3). NO_x concentrations were low; the highest values were recorded at Rancagua city, with hourly concentrations of approximately 40 ppb (Figure 1). The town of Marchigue, a rural town located approximately 38 km east of the Pacific Ocean, showed a low O_3 atmosphere due to consistent onshore sea breezes (southwesterly) during the day. In Rancagua, Codegua, and Rengo, the winds were also predominately from the southwest, with speeds of 2–4 m/s during the period of highest O_3 formation. The low observed concentrations confirmed that the Santiago Basin would not be greatly affected by pollution generated in the Rancagua Valley, whose largest city (Rancagua) has a population of approximately 214,000 inhabitants (Table 1).

3.2. VOCs in Urban and Rural Atmospheres

[30] The VOCs speciation showed that the organic compositions of the three valleys were similar. In Figure 4, the mean normalized hydrocarbon speciation analysis provides a signature of typical dominant traffic emissions (6:00–10:00 LT), which allow comparison between different sites [*Fujita et al*., 1994]. We observed some differences between Santiago Downtown, Las Condes, and Colina with respect to the patterns of 2,3-dimethylbutane and 2,2,4-trimethylpentane (Figure 4a). Peñaflor, a suburban town, exhibited some differences, especially related to biogenic isoprene.

[31] Meanwhile, Figure 4b shows the mean normalized hydrocarbon speciation of Santiago Downtown, Las Condes, and Colina (environmental mean) as compared with exhaust emissions from light-duty vehicles and emissions from diesel buses. The environmental pattern coincided with the typical light-duty vehicle emissions (e.g., 2, 3-dimethylbutane, 2,2,4-trimethylpentane, benzene, toluene, and xylene). It was also possible to distinguish differences between the environmental patterns and exhaust emissions from light-duty vehicles regarding propane. The important environmental presence of propane is perhaps attributable to liquefied petroleum gas. However, a minor difference was observed between the environmental and diesel emission pattern. Other possible sources with similar profiles were not investigated.

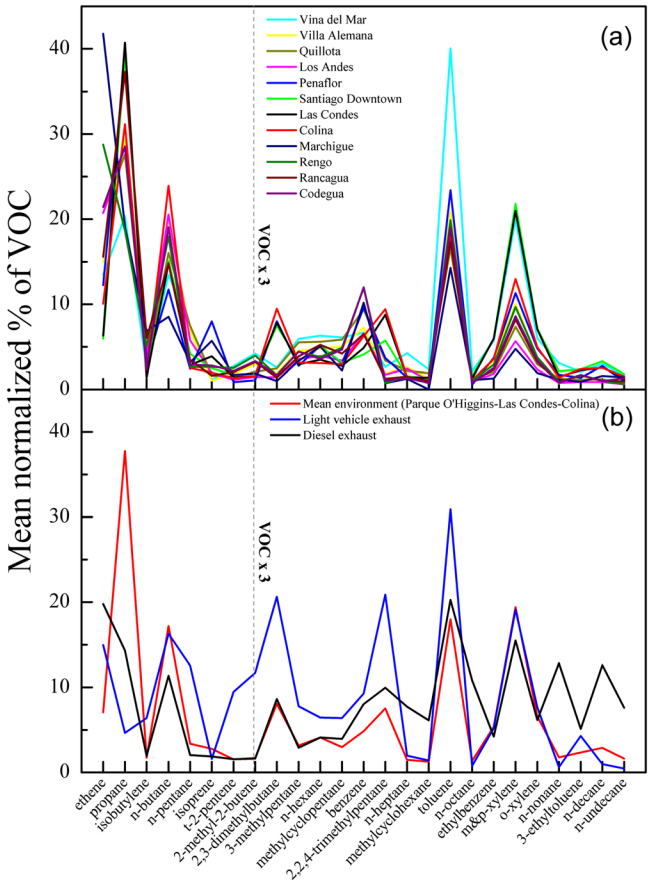

Figure 4. Mean (6:00–10:00 LT) normalized hydrocarbon speciation [*Fujita et al.*, 1994]. To the right of 2-methyl-2-butene, the percentage of the organic species was amplified by a factor of 3 to provide a better visualization. (a) The 12 sites studied, (b) the means found in light-duty vehicle underground parking lots and diesel bus depots and the means in Santiago Downtown, Las Condes, and Colina.

[32] By using the maximum incremental reactivity (MIR) scale, ethene, propene, xylene, and toluene were all identified as the most relevant to ozone formation. Figure 5 shows the theoretical production of ozone associated with the five organic species with greatest ozone-forming potential according to the MIR reactivity scale [*Carter*, 1994]. It is generally true that in the morning hours, the mixture of reactive organic compounds is stagnant below the thermal inversion defining the locations of the highest fresh emissions of photochemical precursors. Consequently, Santiago stands out for being responsible for most of the theoretical productivity of ozone that will impact downwind areas. Next in ozone production importance are Villa Alemana, Viña del Mar, and Las Condes.

[33] The ratio of reactive organic gases (ROG) (e.g., xylene: benzene), frequently used as a surrogate for traffic emissions when vehicle exhaust and evaporative losses during storage and refueling are dominant sources, represents an adequate quantity to describe the photochemical activity due to the different oxidation rates of specific hydrocarbons with the OH radical [*Rappenglück et al.*, 1998].

$$^{\bullet}\mathrm{OH} + \mathrm{VOC} \rightarrow \mathrm{Products} \quad (1)$$

[34] Although this oxidation reaction (kinetic reactivity) does not account for the O_3 generated through reactions that occur afterward (mechanistic reactivity), it allows one to differentiate between regions that have greater levels of "fresh emissions" (relatively high ROG ratios) and those with higher proportions of photochemically aged air (relatively low ratios). Therefore, the xylene:benzene ratio demonstrates the photochemical activity intensity of a specific atmosphere. At higher activity levels, the ratio will be lower due to a higher xylene gas-phase reaction rate with OH at 298 K and 1 atm (m-xylene: $k_{OH} = 23.6 \cdot 10^{-12}\,\mathrm{cm^3\,molecule^{-1}\,s^{-1}}$; p-xylene: $k_{OH} = 14.3 \cdot 10^{-12}\,\mathrm{cm^3\,molecule^{-1}\,s^{-1}}$) compared with that of benzene ($k_{OH} = 1.2 \cdot 10^{-12}\,\mathrm{cm^3\,molecule^{-1}\,s^{-1}}$) [*Atkinson*, 1990]. For example, assuming an OH concentration of $3.5 \cdot 10^6$ molecules $\mathrm{cm^3}$ [*Apel et al.*, 2010], together with the

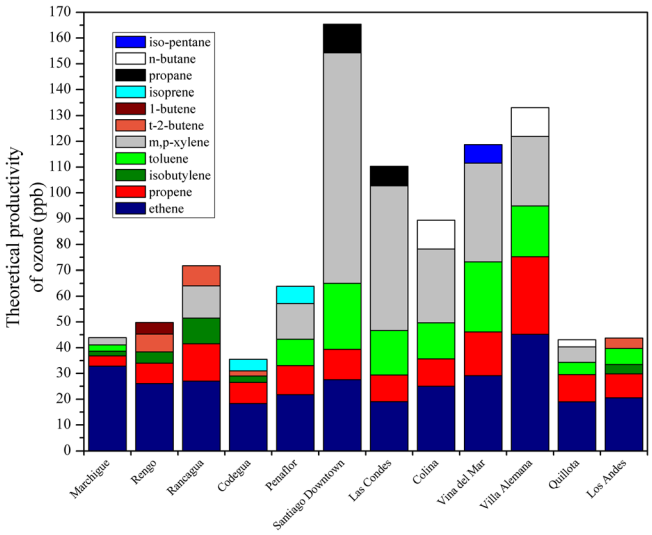

Figure 5. Theoretical productivity of ozone calculated with the MIR scale for five reactive organic gases in the morning (6:00 to 10:00 LT).

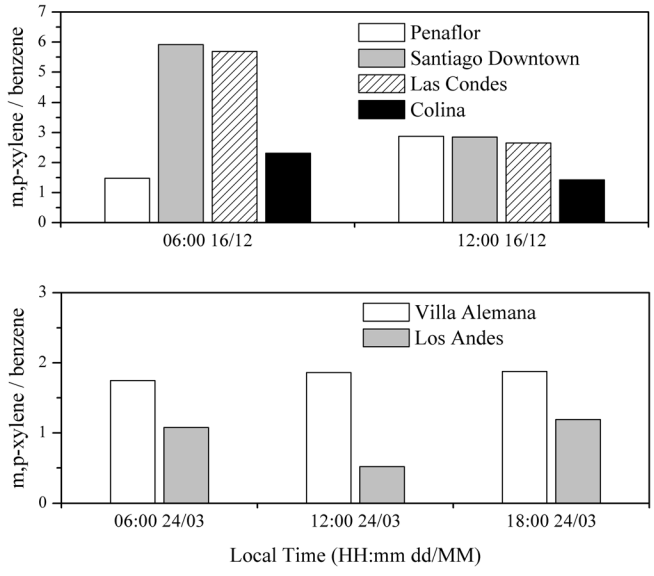

Figure 6. The m,p-xylenes:benzene ratios measured at (a) the Santiago Basin and (b) Villa Alemana and Los Andes.

known OH rate constants, we can estimate the chemical lifetimes for m,p-xylene species to be 3–6 h during regional scale ozone episodes in the Santiago Basin.

[35] Figure 6 shows the changes in m,p-xylene:benzene ratios that correspond to the Santiago Basin during two times of day. Generally, in downtown Santiago, Las Condes, and Colina, the lowest ratios occurred between 12:00 and 16:00 LT, indicating that these sites receive aged air masses from upwind during this period. Additionally, the ML growth can also contribute to decrease the ratio by the vertical mixing of aged contaminants from aloft. Conversely, in Peñaflor, the ratio increases between 12:00 and 16:00 LT, reaching values similar to those found in downtown Santiago and Las Condes, suggesting a possible nighttime precursor recirculation through the RL. This statement can be supported by the identification of an RL in Peñaflor at 14:00 h (Figure 8).

[36] In the Valparaíso Region, there were no significant changes in the m,p-xylene:benzene ratios in Villa Alemana, suggesting no significant photochemical depletion. In contrast, the ratios in Los Andes demonstrate the arrival of photochemically aged air after midday (Figure 6). Subsequently, the ratio increased again during the period corresponding to rush hour and increased vehicle emissions (18:00 to 22:00 LT).

3.3. Vertical Profile of O_3 within the ML

[37] The vertical gradient of ozone concentration has a high diurnal variability. These variations are mainly due to four processes:

(i) Deposition and the titration reaction with NO (reaction (2)), which typically results in nightly depletions [*Zhang and Rao*, 1999].

$$NO + O_3 \rightarrow NO_2 + O_2 \quad (2)$$

As shown in Figure 7, at 6:00 LT, there is almost zero ozone concentration near the surface at all six sites,

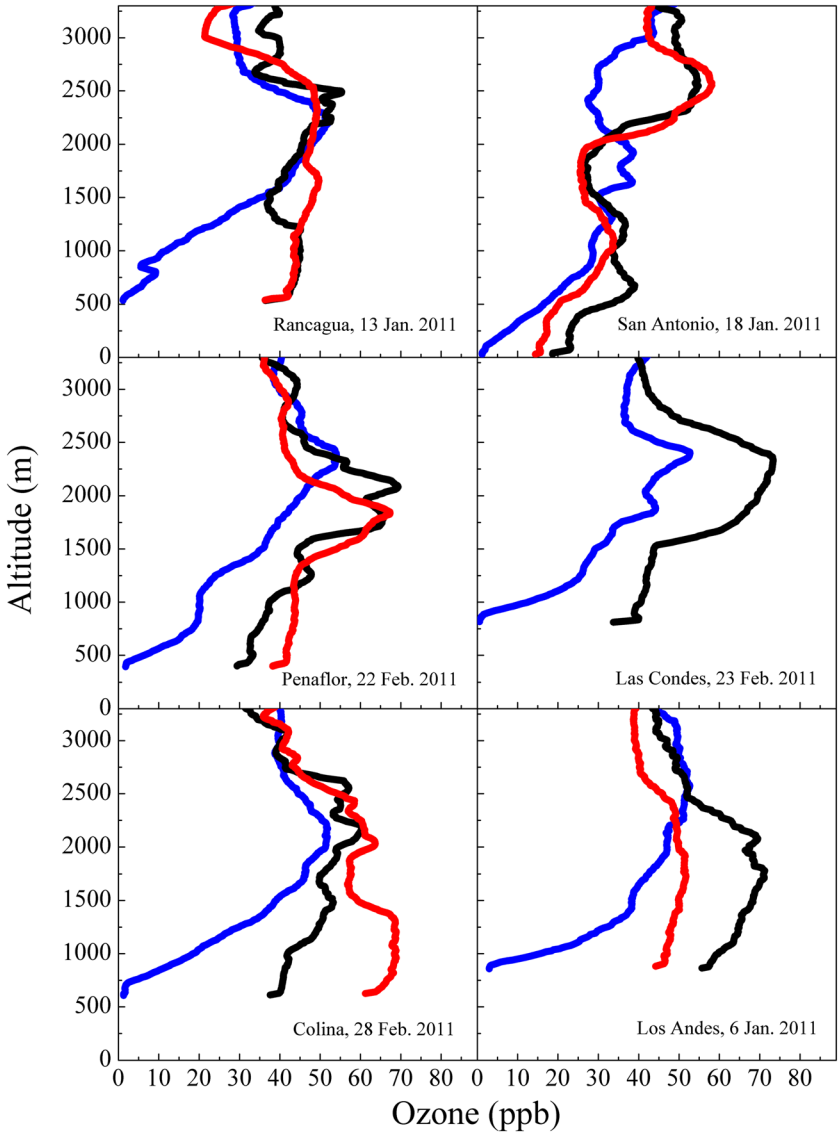

Figure 7. Ozone vertical profiles, from three-launch sequence at 6:00 LT (blue lines), 11:00 LT (black lines), and 14:00 LT (red lines).

with O_3 increasing vertically (~30 to 40 ppb/km), showing that processes that deplete ozone near the surface are very efficient during the night.

(ii) Vertical mixing within the ML. During daytime, surface solar heating generates turbulent eddies that shift the base of the thermal inversion, forming a ML [*Stull*, 1988]. Figure 7 shows that the ozone remains aloft until the growth of the ML. In cases where the RL remains without being completely entrained by the growing ML (in this case Peñaflor, Colina, and Las Condes in Figure 7), the ozone concentration intensifies within the RL probably due to the presence of precursors which trigger a rapid photochemistry that lead to ozone formation. This ozone can be transported within the RL with little dilution as we see in section 3.4.

(iii) In situ photochemical O_3 production from the conversion of NO to NO_2 by reaction with peroxy radicals followed by NO_2 photolysis:

$$RO^{\bullet}_2 + NO \rightarrow RO^{\bullet} + NO_2 \quad (3)$$

$$HO^{\bullet}_2 + NO \rightarrow {}^{\bullet}OH + NO_2 \quad (4)$$

(iv) Transport from upwind sources. Figure 8 shows variations in the ozone profiles from the coastal plain (San Antonio) to the inland areas located upwind and downwind from Santiago like Peñaflor and Colina, respectively. These differences yield important insights for the determination of baseline values. However, the analysis must be considered a qualitative one because a greater number of samplings are required in San Antonio and Peñaflor.

[38] In San Antonio, the increasing wind speed in the afternoon due to the sea breeze is associated with relatively low ozone concentrations. Thus, air masses arriving at San Antonio from the ocean are relatively unpolluted showing

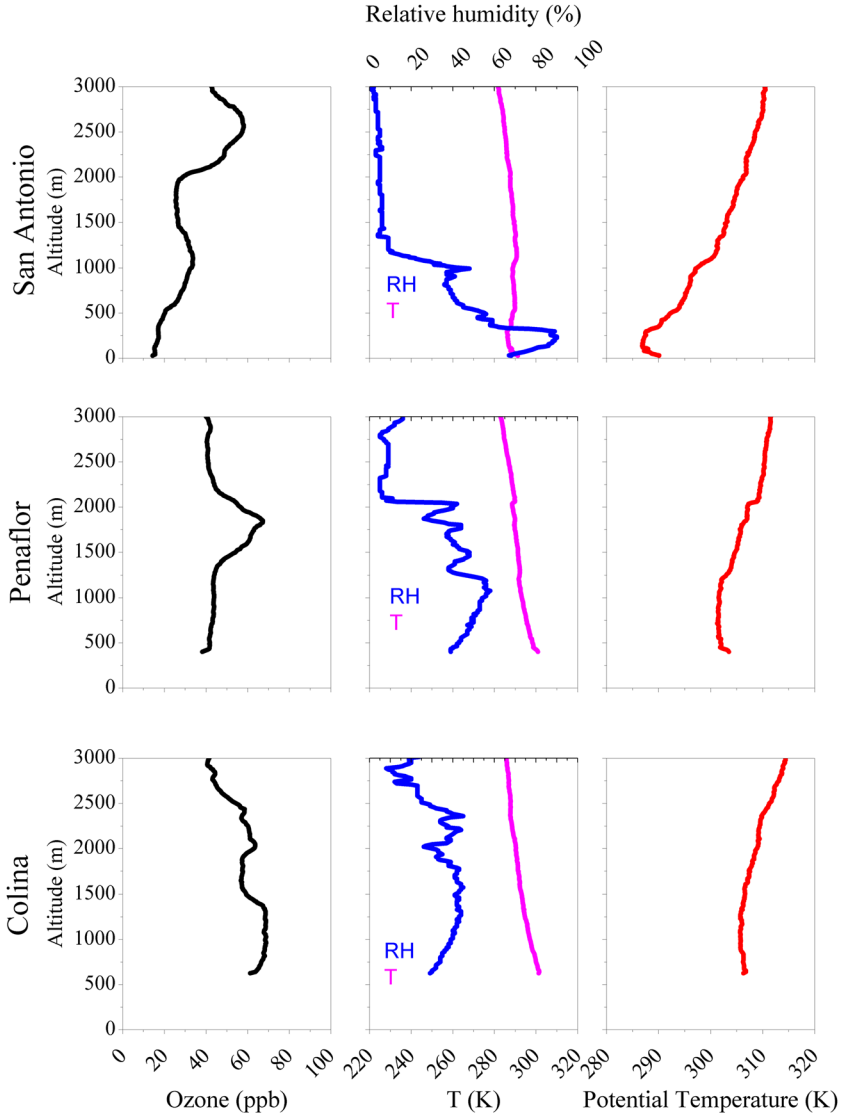

Figure 8. Vertical profiles over San Antonio, Peñaflor, and Colina. The measurements were performed on 18 January (San Antonio), 22 January (Peñaflor), and 28 February 2011 (Colina) at ~14:00 LT, under typical summertime conditions.

lowered ozone mixing ratios in the remote marine boundary layer as described by *Johnson et al*. [1990]. Therefore, it is possible that upwind background ozone concentrations within the ML (below 0.3 km) are mostly determined by coastal air, which is relatively poor in ozone. The background concentrations range from 15 to 25 ppb (Figure 8), which are lower than the values found in the free troposphere (for instance, Figure 9).

[39] On the other hand, the vertical probing of Peñaflor showed that the ozone concentrations were higher than the coastal values. In Peñaflor, the O_3 concentration in the ML did not exceed 45 ppb, in agreement with background values found in the free troposphere (Figure 9). Nevertheless, these concentrations can greatly influence the air quality of Santiago. Complementary to this, the ground level analysis of organic precursors showed important anthropogenic contributions in this location. Toluene (1.0 ± 0.5 ppb) and xylenes (0.74 ± 0.21 ppb) showed higher mixing ratios than would be expected for a suburban location. Also, these species coexisted with biogenic species like isoprene (0.69 ± 0.37 ppb), which has high ozone-forming potential. Finally, Figure 8 shows the ML of Colina with a great abundance of ozone as expected for a location downwind from Santiago City.

[40] Other factors that affect the vertical gradient of ozone include topographic features, since the circulation in the northeastern part of Basin is strongly modulated by the presence of the Andes Mountain. The convective activity due to heated slopes can potentially intensify the ozone contribution aloft in contrast to the western part of the valley where the marine influence can be more important. For example, in Peñaflor, the high RH at noon (~75%) and the relatively higher ozone concentration aloft may mean the undercutting of the ML by clean marine air during sea breeze flow regimes as described by *McElroy and Smith* [1993, and references therein].

3.4. Elevated Ozone Concentration within the RL

[41] Layers of well-aged pollutants aloft [*Blumenthal et al*., 1977; *McElroy and Smith*, 1993] have been observed in Los Angeles (California, USA), a coastal region that has geographic, topographic, and climatological similarities to the Central Zone of Chile. In Santiago, located far enough from the coast (~90 km), the ventilation by clean marine air is poor, and one important mechanism that drives the polluted layers is the strong scale subsidence which favors the stratification of ozone between the subsidence inversion and the ML. Within these stratifications, large abundances of ozone were observed that can potentially affect the ground-level concentrations.

[42] An example of large ozone concentrations in the RL is illustrated by 2 days of soundings performed at Colina on 21 and 22 December 2010 (Figure 9). On 21 December, synoptic conditions showed the presence of a midtropospheric ridge and associated subsidence over Central Chile. In the lower troposphere up to about 5 km, a predominantly southerly wind was observed, which is typically associated with a migratory

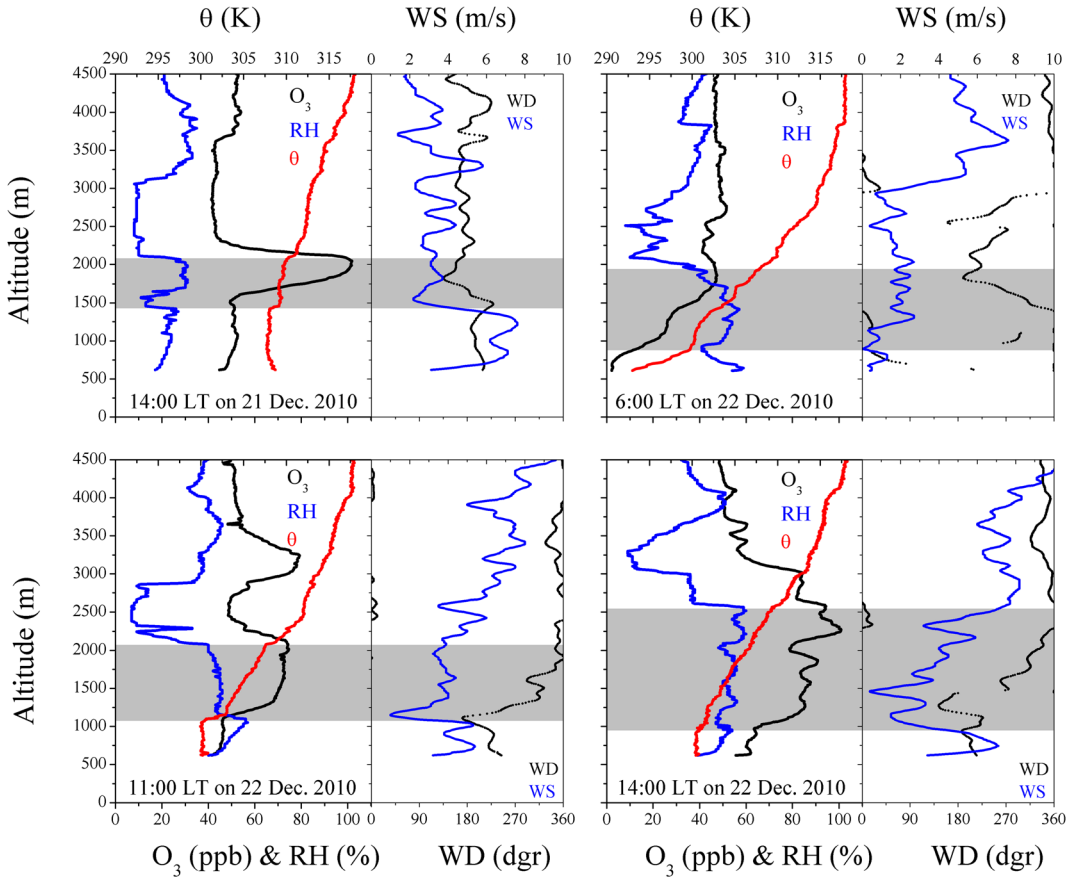

Figure 9. All sonde data from four-launch sequence on 21 and 22 December at Colina. The figure includes potential temperature (θ), relative humidity (RH), O_3 profile, wind speed (WS), and wind direction (WD). The gray zone indicates the RL.

high-pressure system. The ozone was confined above the ML (~1.4 km) and below the subsidence inversion base (~2.1 km). The ozone trapped there reached a maximum concentration of 102 ppb at 2 km asl and potentially can be transported large distances (at a speed of ~3 m/s). Whether this ozone can affect surface concentrations will depend upon vertical mixing along its trajectory.

[43] On the following day (22 December 2010), the passage of the midtropospheric ridge and the approach of a midtropospheric trough resulted in a subsidence inversion base approximately 450 m higher than the previous day. The measurement sequence corresponding to 6:00, 11:00, and 14:00 LT on 22 December 2010 shows subsidence at 2.0, 2.1, and 2.6 km, respectively (Figure 9). The wind direction showed a transition at 6:00 LT. The most noticeable change was observed above 3 km, where the winds returned back to northerly (which is the climatological condition at this level due to the barrier effect of the Andes).

[44] The vertical profile at 6:00 LT shows the typical decrease in the O_3 concentration as a result of the nightly depletions and absence of photochemical processes and transport.

[45] The profile at 11:00 LT shows two maxima of O_3 (Figure 9): the maximum of 75 ppb associated with the RL between 2.0 and 1.0 km and an unexpected maximum of O_3 at ~3.2 km (~79 ppb) above the RL and the subsidence inversion which is associated with northerly wind and accompanied by approximately 40% humidity above 2.9 km. A possible influence by downward mixing from the upper troposphere might be argued, but the humidity associated with the O_3 layer is too high to suggest a stratospheric origin. Rather, the most likely explanation might be the formation of ozone due to remnant precursors generated the previous day which have been recirculated by mountain venting similar to what *McKendry et al.* [1997] describes for Fraser Valley (BC) and *Edinger and Helvey*, [1961] for Los Angeles, where the slope winds are able to inject material above the inversion by convective flow along the heated slope and then advection back over the basin. We believe this process is occurring along the Colina-Los Andes corridor (we will discuss this further in the next section).

[46] Finally, at 14:00 LT, the weakening of the subsidence inversion raised up the base to 2.6 km, thus favoring the mixing of both O_3 maxima, previously observed at 11:00 LT, to generate a deeper layer of relatively high ozone. The further downmixing of this deeper layer also resulted in even higher surface concentrations than the ones recorded the previous day.

3.5. The Role of the RL in the O_3 Transport throughout Colina-Los Andes Corridor

[47] The vertical profiles through the Colina-Los Andes atmospheric corridor are shown in Figure 10. The profile over Colina on 19 January 2011 at 10:53 LT revealed a ML top at

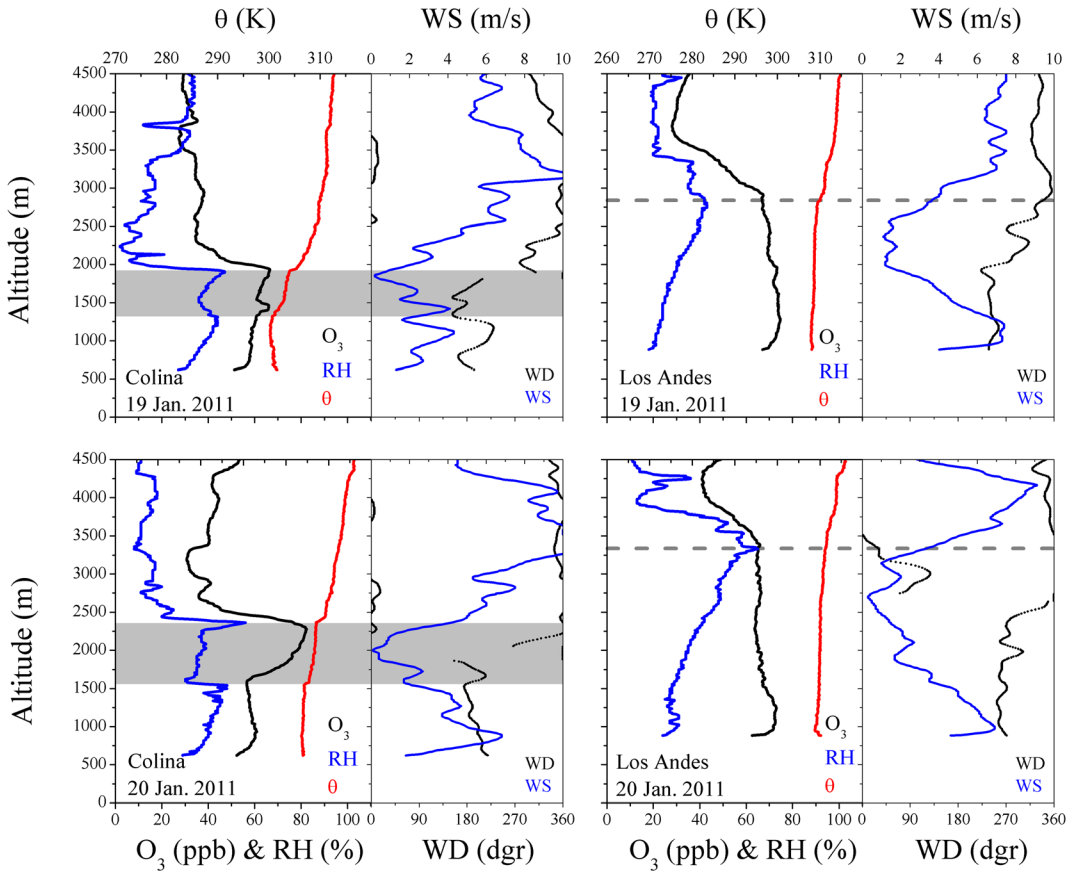

Figure 10. All sonde data from two-launch sequence on 19 January and two-launch sequence on 20 January both at Colina-Los Andes. The figure includes potential temperature (θ), relative humidity (RH), O_3 profile, wind speed (WS), and wind direction (WD). The gray zone indicates the RL, and the gray dashed line indicates the ML height.

1.4 km and a subsidence inversion based at 1.9 km. As seen in Figure 10, higher levels of ozone were identified below 1.9 km. The direction of the wind below ~2.0 km was predominantly southerly (toward the Aconcagua Valley).

[48] During the same day, the profiles in Los Andes at 17:11 LT showed a deep ML (2.8 km); the RL was virtually nonexistent at this time of the day. The subsidence inversion base was higher than in Santiago (~3.5 km) probably due to the topographic feature, altitude, and the slope fluxes. Therefore, the ozone was distributed relatively homogeneously in the vertical (Figure 10). The direction of the wind below 2.5 km was southwesterly.

[49] Figure 11 shows the surface ozone concentrations at Colina, Chacabuco slope, and Los Andes for the same day (19 January 2011). The Los Andes curve shows that during the morning, the ozone was not titrated with the same efficiency as it was in Colina through reaction (2). This can be explained as an excess of O_3 with respect to NO. A second distinguishing feature is the advancement of the ozone accumulation period, which begins 2 h earlier in Los Andes than it does in Colina. The difference in timing can be due to the lower inhibition caused by NO_x emissions in VOC-limited regimes during the morning hours. Lower NO emissions decrease the titration of O_3. At the same time, lower concentrations of NO_2 consuming OH (5) lead to greater availability of OH radicals to react with VOCs through reaction (1) and to subsequently form O_3 according to reactions (3) and (4).

$$^{\bullet}OH + NO_2 + M \rightarrow HNO_3 + M \quad (5)$$

[50] *Fujita et al.* [2003] found that in the southern coast of California, the time of accumulation occurs an hour earlier during the weekends compared to weekdays, when lower emissions of NO_x occur.

[51] In addition to the above discussion, other factors (not discussed) that include meteorological conditions (e.g., wind speed) could explain these differences.

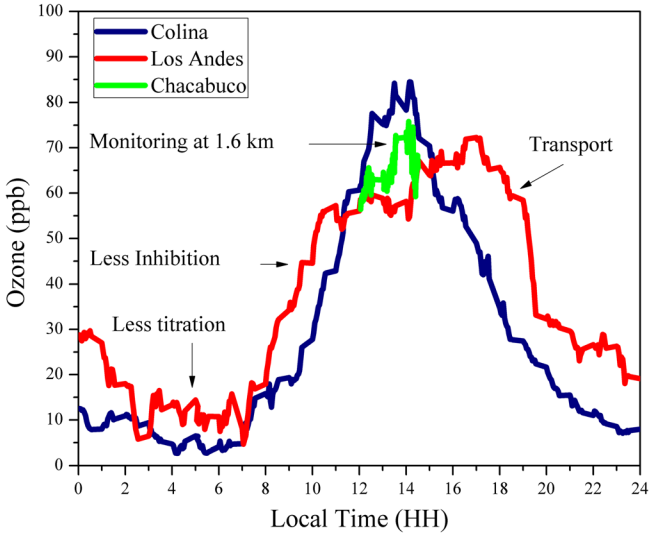

Figure 11. Diurnal variations of O_3 on 19 January 2011 in Colina and Los Andes, along with monitoring at 1.6 km conducted at the Chacabuco mountain range.

[52] However, at Los Andes, the greater amplitude of the ozone concentrations in the afternoon is indicative of the arrival of air that is rich in ozone (Figures 11 and 1). For example, the wind speed taken from the sounding launched on 19 January at Los Andes (Figure 10) was 2.2 m/s at 1.9 km, and the distance between Colina and Los Andes is 41 km, implying it takes an air parcel approximately 5 h to arrive at Los Andes. Figure 11 shows that, from the time that the maximum ozone concentration of 72 ppb was recorded in Colina at 12:45 LT, a total of ~5 h passed until the maximum ozone levels were recorded in Los Andes at 17:15 LT.

[53] The tethersonde measurements at the peak of La Cruz hill, located in the Chacabuco mountain range, enabled the recording of O_3 concentrations at an altitude of approximately 1.6 km. The high concentrations measured on 19 January, with a maximum of 76 ppb (13:15 LT), suggest that the photochemical smog produced in the Metropolitan Region is capable of traveling across the Chacabuco range considering the timing between the maximum in Colina and Los Andes and also the fact that no local sources are known for the Chacabuco range rural area.

[54] The phenomenon described in this section (19 January 2011) was also observed on 20 and 21 January. For instance, a deeper RL was identified in Colina on 20 January, while the same deep ML was developed in Los Andes (Figure 10). Similarly, the widening in the diurnal cycle of ozone was observed in the afternoon (not shown).

[55] To strengthen the links between Santiago City influx and Los Andes convergence zone, analyses of back trajectories were performed during the same period (19, 20, and 21 January) using output from the WRF model. Trajectories support the idea that transport occurs during the daytime within the RL and the growing mixed boundary layer. Trajectories originating in the Santiago Basin, 3–7 h earlier and between 1.2 and 2 km, are able to reach Los Andes (Figures 12c and 12d) from about 19 January 2011, 13:00 to 24:00 LT. Winds tend to be stronger along trajectories reaching Los Andes during evening hours as shown by the longer path followed by the trajectories (Figure 12e). Well above the mixed boundary layer, trajectories are mostly influenced by the blocking flow with a northerly component induced by the Andes [*Kalthoff et al.*, 2002] and less affected by the local mountain-valley circulations. A similar behavior of the daily cycle of the trajectories is observed during the 3 days simulated.

[56] Given the relatively small influence of synoptic scale variability especially in the surface circulation, we regard these trajectories as broadly representative of summertime conditions within the region of study. We hypothesize that the increase in ozone around 14:00 LT (Figure 11) is explained by the arrival of parcels originated in the Santiago Basin loaded with ozone and precursors and subsequently mixed from above by the growing boundary layer over Los Andes. The rapid decline in surface ozone at Los Andes at ~19:00 LT is not explained by the back trajectories, since transport of parcels from the Santiago Basin continues within the RL up until midnight. Rather, this decline at ground level can be explained by the change of wind direction. Indeed, the valley-mountain breeze typically turns to the northeast direction after 19:00 LT. However, the effect of the transport to Los Andes from Santiago during the evening hours might also help to explain the

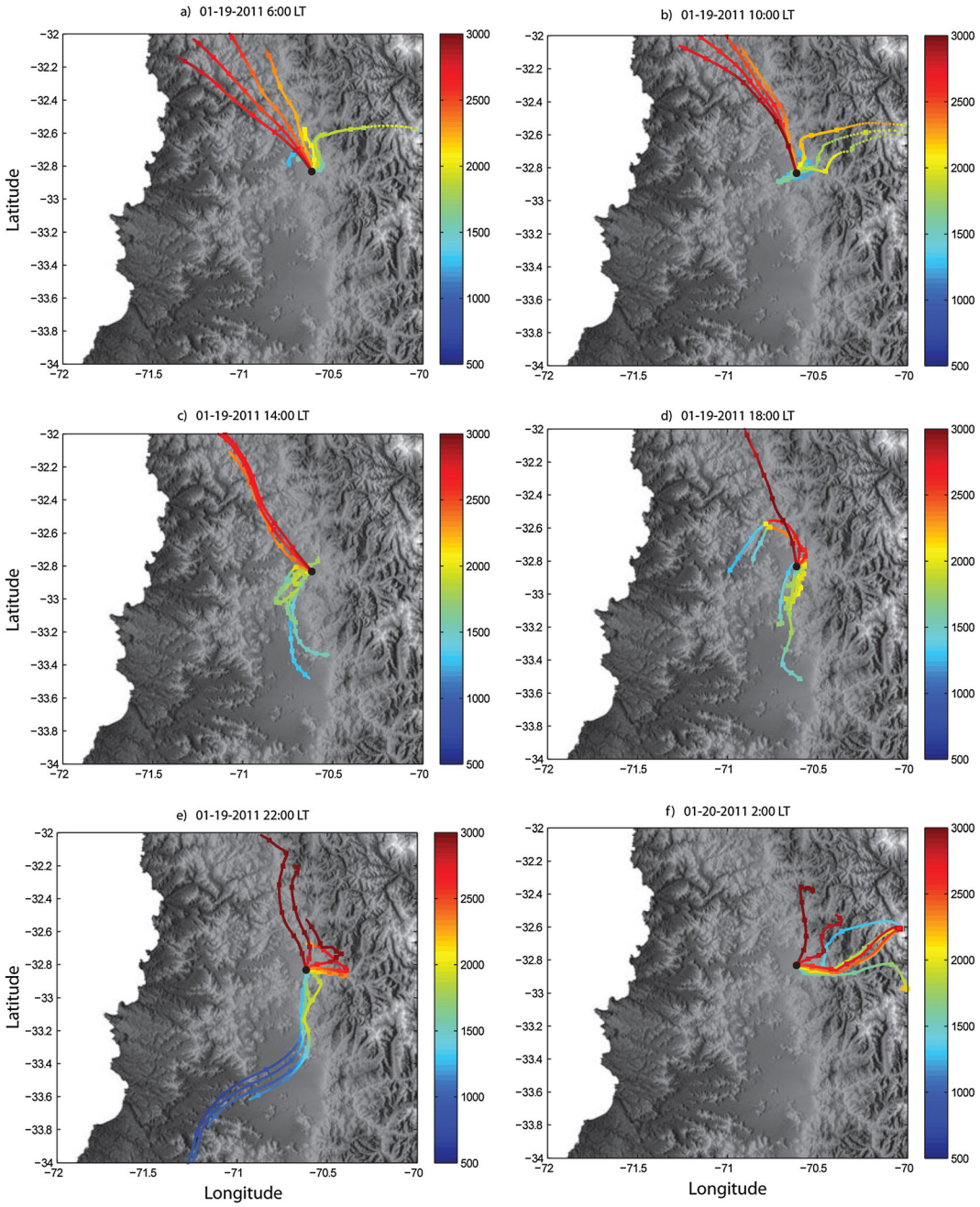

Figure 12. Back trajectories ending at Los Andes during 19–20 January 2011. The trajectories end every 200 m in the vertical from 1.3 km to 2.9 km asl The colors represent the height of the particular trajectory. Back trajectories are about 7 h long. Each hour is identified by a larger dot in the trajectory, so longer trajectories represent relatively strong winds along the trajectories.

rapid increase in ozone during the morning hours of the following day.

[57] Finally, the information collected through this study allows us to propose a model of ozone recirculation for Santiago Basin and the east of the Aconcagua valley; the ozone from layers aloft, mainly through the RL, are transported from Santiago to Los Andes and are vertically mixed up to ~3.5 km. As over ~3 km the wind is predominantly from the north due to the blocking flow induced by Los Andes range, the ozone at this altitude is advected back over the capping inversion of Santiago. This model would explain the ozone maximum observed at ~3.2 km over Colina at 11:00 LT (Figure 9).

4. Conclusions

[58] Surface monitoring conducted in the Chilean Central Valleys demonstrated that the horizontal gradients of NO_x and VOC are mainly related to the proximity of emission and transport sources in the direction of the predominant winds. Santiago and Villa Alemana are notable for having relatively high concentrations of NO_x and VOC; however,

the greatest concentrations of ozone were found in Las Condes, Colina, and Los Andes, located downwind from the sources.

[59] Ozone concentrations in the "entryway" of the Santiago Basin (Peñaflor) did not exceed 45 ppb within the mixing layer. Nevertheless, this background concentration leaves a narrow margin for ozone formation without exceeding the standard value of 61 ppb in the Santiago Basin. In contrast, low O_3 concentrations in the Rancagua Valley and the predominant wind direction support the claim that Santiago Basin is not presently affected by secondary contaminants from the Rancagua Valley.

[60] Nighttime surface O_3 concentrations in the valleys typically decreased to zero, whereas in higher areas (approximately 800 m), such an extreme decrease was not observed (e.g., in Los Andes).

[61] The m,p-xylene:benzene ratios show that between 12:00 and 16:00 LT, downtown Santiago, Las Condes, Colina, and Los Andes all receive photochemically aged air masses. Consistent with the profile data, these ratios indicate that the growth of the ML at 11:00 and 14:00 LT favors the entrainment of O_3-rich aged and contaminated air from the RL.

[62] The RL provides a transport route to convergence sites with good vertical mixing. Over Santiago Basin, large-scale subsidence conditions that prevail all year-round in this region favor the stratification of ozone over the ML and below the base of the subsidence inversion. O_3 stratifications of up to 102 ppb at 2.0 km were found in the RL. Los Andes was identified as a typical convergence zone for ozone in the RL, where subsequent vertical down-mixing during daytime contributes to ozone concentrations at the surface. This is also supported by the analysis of back trajectories performed for 3 days under typical summertime conditions.

[63] Since the focus of this work was mostly observations, several questions remain open that call for the use of chemical transport models. In particular, we believe the application of photochemical models to reproduce the observed variability in the surface and vertical data would help to better understand ozone formation and transport. Also, it would be important for developing effective control strategies.

[64] **Acknowledgments.** The authors wish to thank the anonymous reviewers for their critical and useful recommendations for improving the paper. We thank R. Sánchez for assistance in the WRF numerical simulation. We also thank M. Falvey for providing software for plotting topography in Figures 1 and 12. This study was supported by the partnership between the Ministry of the Environment and the National Center of the Environment. R. J. S. acknowledges the financial support from BECAS CHILE. This paper was edited by Arthur M. Winer.

References

Altshuller, A. P., and A. S. Lefohn (1996), Background ozone in the planetary boundary layer over the United States, *J. Air Waste Manage. Assoc.*, *46*(2), 134–141.

Apel, E. C., et al. (2010), Chemical evolution of volatile organic compounds in the outflow of the Mexico City Metropolitan area, *Atmos. Chem. Phys.*, *10*(5), 2353–2375.

Athanassiadis, G. A., S. T. Rao, J. Ku, and R. D. Clark (2002), Boundary layer evolution and its influence on ground level ozone concentrations, *Environ. Fluid Mech.*, *2*, 339–357.

Atkinson, R. (1990), Gas-phase tropospheric chemistry of organic compounds: A review, *Atmos. Environ.*, Part A. General Topics, *24*(1), 1–41.

Atkinson, R. (2000), Atmospheric chemistry of VOCs and NOx, *Atmos. Environ.*, *34*(12–14), 2063–2101.

Bell, M. L., A. McDermott, S. L. Zeger, J. M. Samet, and F. Dominici (2004), Ozone and short-term mortality in 95 US urban communities, 1987–2000, *JAMA-J. Am. Med. Assoc.*, *292*(19), 2372–2378.

Blumenthal, D. L., W. H. White, and T. B. Smith (1977), Anatomy of a Los Angeles smog episode: Pollutant transport in the daytime sea breeze regime, *Atmos. Environ.*, *12*, 893–907.

Carter, W. P. L. (1994), Development of ozone reactivity scales for organic gases, *J. Air Waste Manage. Assoc.*, *44*, 881–899.

Chameides, W. L., et al. (1992), Ozone precursor relationships in the ambient atmosphere, *J. Geophys. Res.-Atmos.*, *97*(D5), 6037–6055.

Chameides, W. L., R. W. Lindsay, J. Richardson, and C. S. Kiang (1988), The role of biogenic hydrocarbons in urban photochemical smog: Atlanta as a case study, *Science*, *241*(4872), 1473–1475.

Clough, S. A., M. W. Shephard, E. J. Mlawer, J. S. Delamere, M. J. Iacono, K. Cady-Pereira, S. Boukabara, and P. D. Brown (2005), Atmospheric radiative transfer modeling: A summary of the AER codes, *J. Quant. Spectrosc.Ra.*, *91*(2), 233–244.

Edinger J., and R. Helvey (1961), The San Fernando convergence zone, *Bull. Am. Met. Soc.*, *42*, 626–635.

Fujita, E. M., D. R. Lawson, and C. M. Association (1994), Evaluation of the Emissions Inventory in the South Coast Air Basin: Final Report, Energy and Environmental Engineering Center, Desert Research Institute.

Fujita, E. M., W. R. Stockwell, D. E. Campbell, R. E. Keislar, and D. R. Lawson (2003), Evolution of the magnitude and spatial extent of the weekend ozone effect in California's South Coast Air Basin, 1981–2000, *J. Air Waste Manage. Assoc.*, *53*(7), 802–815.

Janjić, Z. I. (1994), The step-mountain eta coordinate model: Further developments of the convection, viscous sublayer, and turbulence closure schemes, *Mon. Weather Rev.*, *122*(5), 927–945.

Jenkin, M. E., and K. C. Clemitshaw (2000), Ozone and other secondary photochemical pollutants: Chemical processes governing their formation in the planetary boundary layer, *Atmos. Environ.*, *34*(16), 2499–2527.

Johnson, J. E., R. H. Gammon, J. Larsen, T. S. Bates, S. J. Oltmans, and J. C. Farmer (1990), Ozone in the marine boundary layer over The Pacific and Indian oceans: Latitudinal gradients and diurnal cycles, *J. Geophys. Res.-Atmos.*, *95*(D8), 11847–11856.

Kalthoff, N., et al. (2002), Mesoscale wind regimes in Chile at 30°S, *J. Appl. Meteorol.*, *41*(9), 953–970.

Lee, D. S., M. R. Holland, and N. Falla (1996), The potential impact of ozone on materials in the U.K, *Atmos. Environ.*, *30*(7), 1053–1065.

Lippmann, M. (1991), Health effects of tropospheric ozone, *Environ. Sci. Technol.*, *25*(12), 1954–1962.

McConnell, R., K. Berhane, F. Gilliland, S. J. London, T. Islam, W. J. Gauderman, E. Avol, H. G. Margolis, and J. M. Peters (2002), Asthma in exercising children exposed to ozone: A cohort study, *Lancet*, *359*(9304), 386–391.

McElroy, J. L., and T. B. Smith (1993), Creation and fate of ozone layers aloft in Southern California, *Atmos. Environ. A-Gen.*, *27*(12), 1917–1929.

McKendry, I. G., D. G. Steyn, J. Lundgren, R. M. Hoff, W. Strapp, K. Anlauf, F. Froude, J. B. Martin, R. M. Banta, and L. D. Olivier (1997), Elevated ozone layers and vertical down-mixing over the Lower Fraser Valley, BC, *Atmos. Environ.*, *31*(14), 2135–2146.

Morris, G. A., B. Ford, B. Rappenglück, A. M. Thompson, A. Mefferd, F. Ngan, and B. Lefer (2010), An evaluation of the interaction of morning residual layer and afternoon mixed layer ozone in Houston using ozonesonde data, *Atmos. Environ.*, *44*(33), 4024–4034.

Neu, U., T. Kunzle, and H. Wanner (1994), On the relation between ozone storage in the residual layer and daily variation in near-surface ozone concentration—A case study, *Bound.-Layer Meteor.*, *69*(3), 221–247.

Nielsen-Gammon, J. W., C. L. Powell, M. J. Mahoney, W. M. Angevine, C. Senff, A. White, C. Berkowitz, C. Doran, and K. Knupp (2008), Multisensor estimation of mixing heights over a coastal city, *J. Appl. Meteorol. Climatol.*, *47*(1), 27–43.

Pleim, J. E., and A. Xiu (1995), Development and testing of a surface flux and planetary boundary-layer model for application in mesoscale models, *J.Appl. Meteorol.*, *34*(1), 16–32.

Préndez, M., and H. Peralta (2005), Determination of emission factors of volatile organic compounds of two native tree species in Chile's metropolitan region [*Información tecnológica*], *16*, 17–27. Available from <http://www.scielo.cl/scielo.php?script=sci_arttext&pid=S0718-07642005000100004&lng=es&nrm=iso>. ISSN 0718–0764. doi: 10.4067/S0718-07642005000100004.

Rappenglück, B., P. Fabian, P. Kalabokas, L. G. Viras, and I. C. Ziomas (1998), Quasi-continuous measurements of non-methane hydrocarbons (NMHC) in the greater Athens area during MEDCAPHOT-TRACE, *Atmos. Environ.*, *32*(12), 2103–2121.

Rappenglück, B., P. Oyola, I. Olaeta, and P. Fabian (2000), The evolution of photochemical smog in the metropolitan area of Santiago de Chile, *J. Appl. Meteorol.*, *39*(3), 275–290.

Rappenglück, B., R. Schmitz, M. Bauerfeind, F. Cereceda-Balic, D. von Baer, H. Jorquera, Y. Silva, and P. Oyola (2005), An urban photochemistry study in Santiago de Chile, *Atmos. Environ.*, *39*(16), 2913–2931.

Rubio, M. A., P. Oyola, E. Gramsch, E. Lissi, J. Pizarro, and G. Villena (2004), Ozone and peroxyacetylnitrate in downtown Santiago, Chile, *Atmos. Environ.*, *38*(29), 4931–4939.

Schmitz, R. (2005), Modelling of air pollution dispersion in Santiago de Chile, *Atmos. Environ.*, *39*(11), 2035–2047.

Seguel, R. J., R. G. E. Morales, and M. A. Leiva (2009), Estimations of primary and secondary organic carbon formation in PM2.5 aerosols of Santiago City, Chile, *Atmos. Environ.*, *43*(13), 2125–2131.

Seguel, R. J., R. G. E. Morales, and M. A. Leiva (2012), Ozone weekend effect in Santiago, Chile, *Environ. Pollut.*, *162*, 72–79.

Skamarock, W., J. Klemp, J. Dudhia, D. Gill, D. Barker, W. Wang, and J. Powers (2007), A Description of the Advanced Research WRF Version 2 NCAR.

Smit, H. G. J., et al. (2007), Assessment of the performance of ECC-ozonesondes under quasi-flight conditions in the environmental simulation chamber: Insights from the Juelich Ozone Sonde Intercomparison Experiment (JOSIE), *J. Geophys. Res. Atmos.*, *112*, D19306, doi:10.1029/2006JD007308.

Stull, R. B. (1988), An Introduction to Boundary Layer Meteorology, Kluwer Academic.

U.S. EPA (1999), Method TO15: Determination of volatile organic compounds (VOCs) in air collected in specially-prepared canisters and analyzed by gas chromatography/mass spectrometry (GC/MS), in *Compendium of methods for the determination of toxic organic compounds in ambient air*, Second edition, EPA/625/R-96/010b, Office of Research and Development, U.S. Environmental Protection Agency.

Zaveri, R. A., et al. (2010), Overnight atmospheric transport and chemical processing of photochemically aged Houston urban and petrochemical industrial plume, *J. Geophys. Res. Atmos.*, 115, D23303, doi:10.1029/2009JD013495.

Zhang, J., and S. T. Rao (1999), The role of vertical mixing in the temporal evolution of ground-level ozone concentrations, *J.Appl. Meteorol.*, *38* (12), 1674–1691.

Zielinska, B., J. C. Sagebiel, G. Harshfield, A. W. Gertler, and W. R. Pierson (1996), Volatile organic compounds up to C-20 emitted from motor vehicles: Measurement methods, *Atmos. Environ.*, *30*(12), 2269–2286.